A

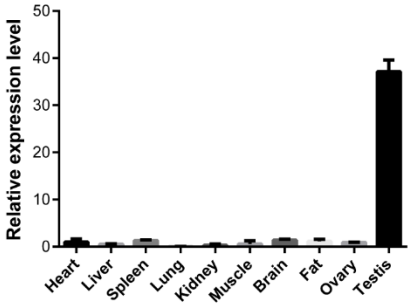
Relative expression level
50
40
30
20
10
0
Heart
Liver
Spleen
Lung
Kidney
Muscle
Brain
Fat
Ovary
Testis

B

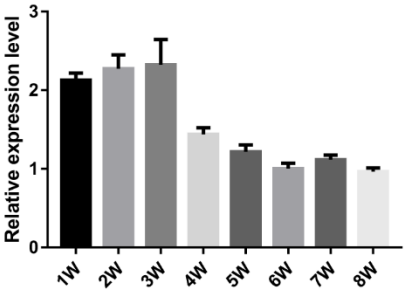
Relative expression level
3
2
1
0
1W
2W
3W
4W
5W
6W
7W
8W

C

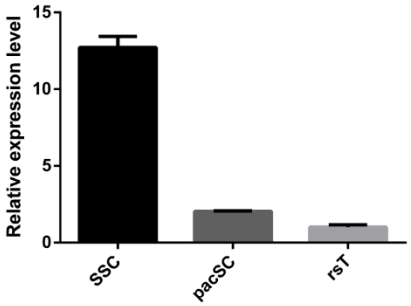
Relative expression level
15
10
5
0
SSC
pacSC
rsT

Supplementary information, Figure S1. *Pnldc1* mRNA is highly enriched in mouse testis.
(A-B) Quantitative RT-PCR analysis for *Pnldc1* mRNA level in various tissues (A) and postnatal mouse testis from 1 week to 8 weeks (B).
(C) *Pnldc1* mRNA level in cultured spermatogonial stem cells (SSCs), isolated pachytene spermatocytes (pacSC) and round spermatids (rST) through STA-PUT method.

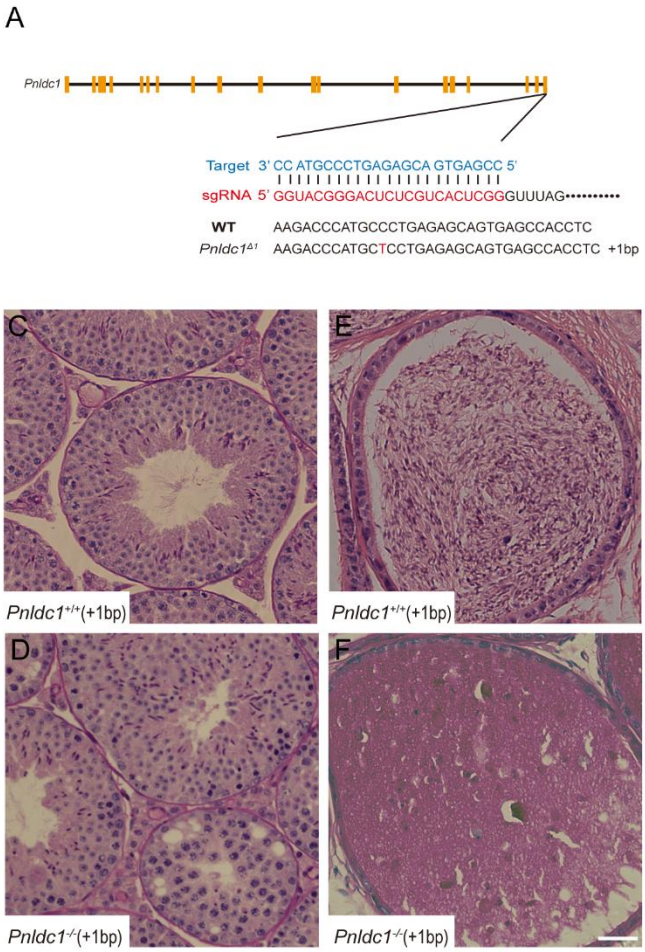
A
Pnldc1
Target 3' CC ATGCCCTGAGAGCA GTGAGCC 5'
sgRNA 5' GGUACGGGACUCUCGUCACUCGGGUUUAG
WT AAGACCCATGCCCTGAGAGCAGTGAGCCACCTC
Pnldc1Δ1 AAGACCCATGCTCCTGAGAGCAGTGAGCCACCTC +1bp
B
Pnldc1+/+
Pnldc1-/-
Testes weight/Body weight (%)
0.5
0.4
0.3
0.2
0.1
0.0
C
Pnldc1+/+(+1bp)
E
Pnldc1+/+(+1bp)
D
Pnldc1-/-(+1bp)
F
Pnldc1-/-(+1bp)

Supplementary information, Figure S2. Phenotype analysis of *Pnldc1* +1bp mouse line.
(A) Schematic diagram of targeting strategy. Upper panel: structure of mouse *Pnldc1* gene on Chromosome 17. The orange box indicates the location of exon. The location of targeted site and the sequence of sgRNA are shown. Lower panel: nucleotide sequence of wild-type allele and sequence analysis of +1bp mutant allele.
(B) Testis weight/body weight ratio of adult $Pnldc1^{+/+}$and $Pnldc1^{+1bp/+1bp}$ mice.
(C,D) Periodic Acid-Schiff (PAS) staining of testis sections from adult $Pnldc1^{+/+}$ and $Pnldc1^{+1bp/+1bp}$ mouse.
(E,F) Hematoxylin-eosin (H-E) staining of epididymides from adult $Pnldc1^{+/+}$ and $Pnldc1^{+1bp/+1bp}$ mice. Scale bar, 50μm.

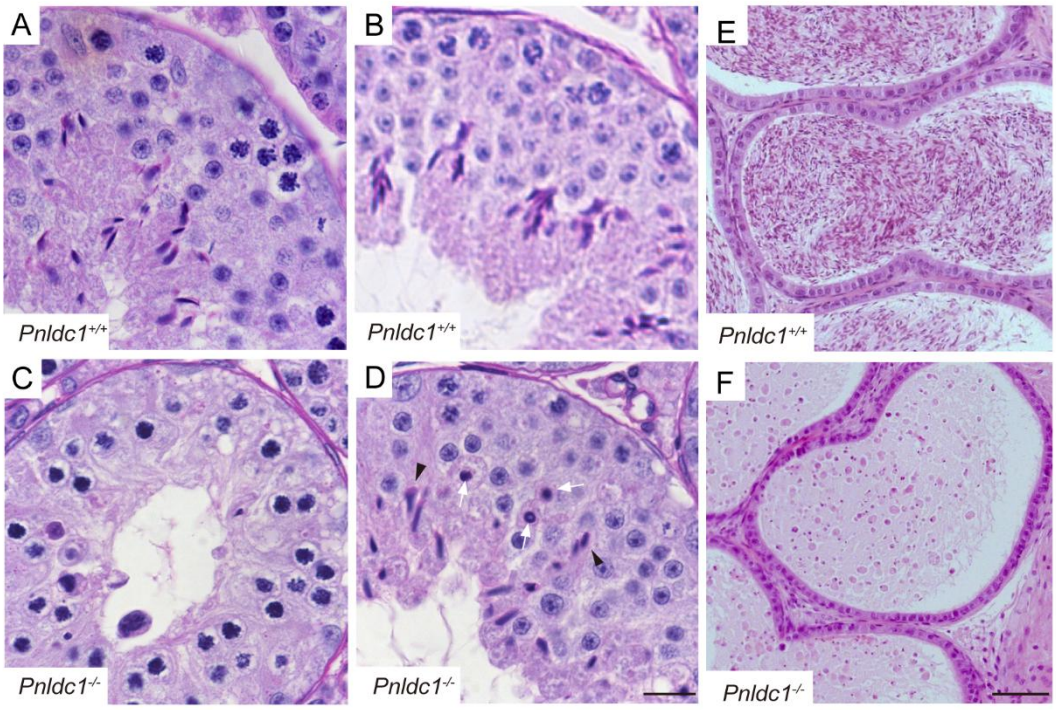
A
B
E
Pnldc1+/+
Pnldc1+/+
Pnldc1+/+
C
D
F
Pnldc1-/-
Pnldc1-/-
Pnldc1-/-

G

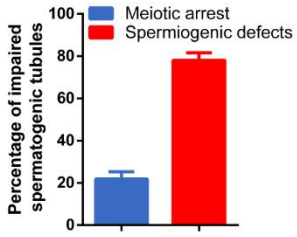
Meiotic arrest
Spermiogenic defects
Percentage of impaired spermatogenic tubules
100
80
60
40
20
0

H

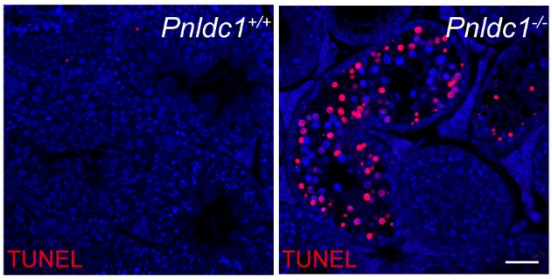
Pnldc1+/+
Pnldc1-/-
TUNEL
TUNEL

I

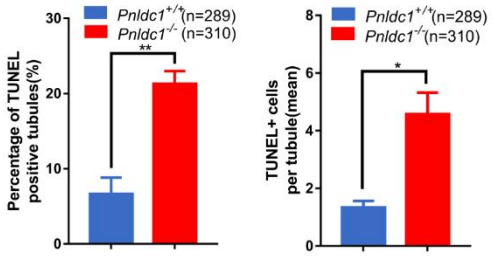
Pnldc1+/+(n=289)
Pnldc1-/- (n=310)
**
Percentage of TUNEL positive tubules(%)
30
20
10
0
Pnldc1+/+(n=289)
Pnldc1-/-(n=310)
*
TUNEL+ cells per tubule(mean)
8
6
4
2
0

Supplementary information, Figure S3. Impaired meiosis and spermiogenesis in *Pnldc1*$^{-/-}$(-7bp) mice.

(A-D) PAS staining of testis sections from adult *Pnldc1*$^{+/+}$mice (A-B) and age matched *Pnldc1*$^{-/-}$ mice (C-D). Abnormal spermatogenic cells were indicated by arrows. Scale bar, 10μm.

(E,F) Hematoxylin-eosin (H-E) staining of epididymides from *Pnldc1*$^{+/+}$ and *Pnldc1*$^{-/-}$ mice at 8- week-old. Scale bar, 50μm.

(G) The proportion for meiotic arrest and spermiogenic defects in the *Pnldc1* mutant testis.

(H) TUNEL assay for *Pnldc1*$^{+/+}$ and *Pnldc1*$^{-/-}$ testes at 8-week-old. Scale bar, 10μm.

(I) Quantification of TUNEL-positive spermatocytes. *P<0.05, ** P<0.01.

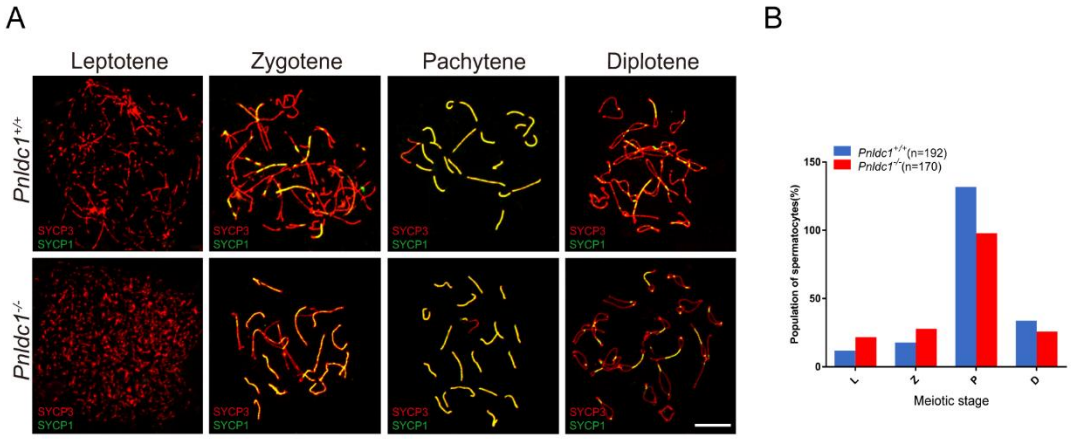
A
Leptotene
Zygotene
Pachytene
Diplotene
Pnldc1+/+
Pnldc1-/-
SYCP3
SYCP1
B
Pnldc1+/+(n=192)
Pnldc1-/-(n=170)
Population of spermatocytes(%)
150
100
50
0
L
Z
P
D
Meiotic stage

Supplementary information, Figure S4. *Pnldc1*$^{-/-}$ mice exhibited defects in meiotic progression.

(A) Immunostaining of nuclear spreads using antibodies against SYCP3 and SYCP1. Scale bar, 10μm. Different meiotic stages of spermatocytes were identified based on immunostaining pattern of SYCP1 and SYCP3.

(B) Percentages of indicated meiotic stages of spermatocytes in *Pnldc1*$^{+/+}$ and *Pnldc1*$^{-/-}$ testes at 8-week-old.

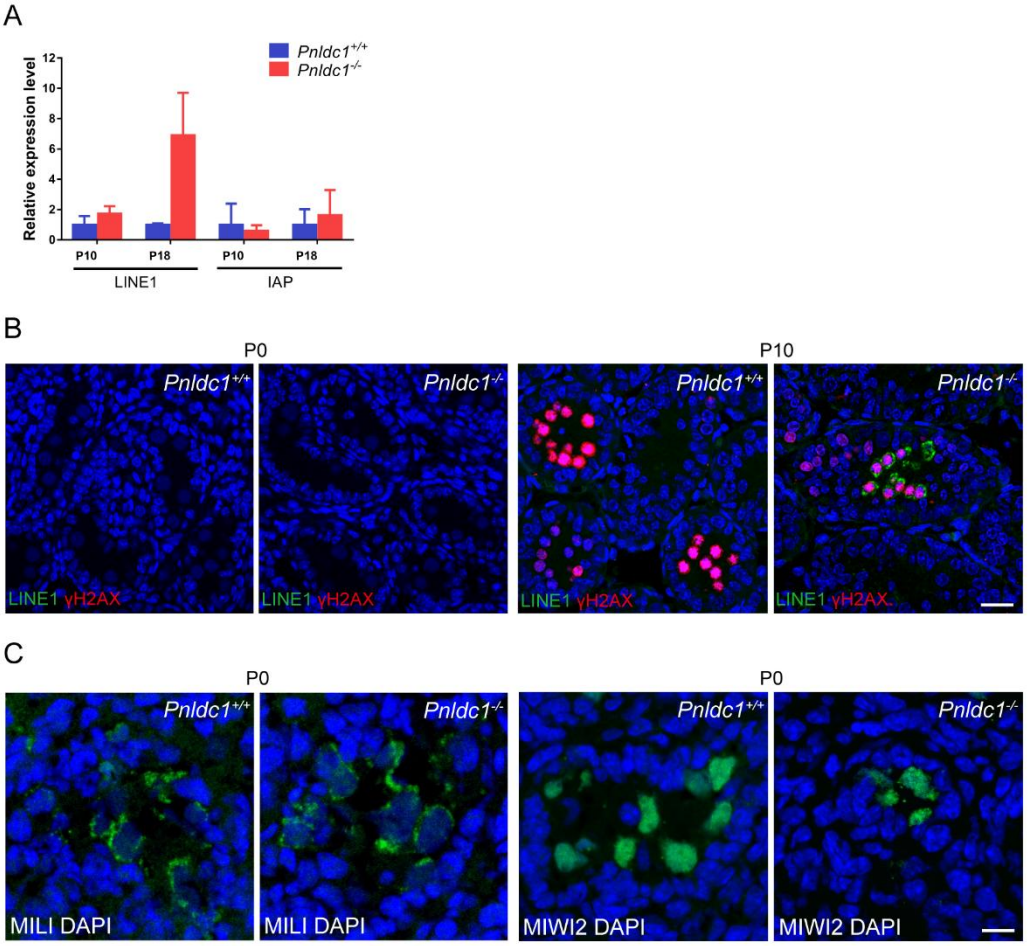
A
Pnldc1+/+
Pnldc1-/-
Relative expression level
12
10
8
6
4
2
0
P10
P18
P10
P18
LINE1
IAP
B
P0
P10
Pnldc1+/+
Pnldc1-/-
Pnldc1+/+
Pnldc1-/-
LINE1 γH2AX
LINE1 γH2AX
LINE1 γH2AX
LINE1 γH2AX
C
P0
P0
Pnldc1+/+
Pnldc1-/-
Pnldc1+/+
Pnldc1-/-
MILI DAPI
MILI DAPI
MIWI2 DAPI
MIWI2 DAPI

Supplementary information, Figure S5. LINE1 retrotransposons were de-repressed in *Pnldc1*$^{-/-}$ Testes.

(A) LINE1 and IAP mRNA transcripts in *Pnldc1*$^{+/+}$ and *Pnldc1*$^{-/-}$ testes at P10 and P18 by quantitative RT-PCR.

(B) Immunofluorescence detection of L1ORF1p in P0 and P10 *Pnldc1*$^{+/+}$and *Pnldc1*$^{-/-}$ testes. Scale bar, 20μm.

(C) Immunofluorescence detection of MILI and MIWI2 in P0 *Pnldc1*$^{+/+}$and *Pnldc1*$^{-/-}$ testes. Scale bar, 20μm.

A

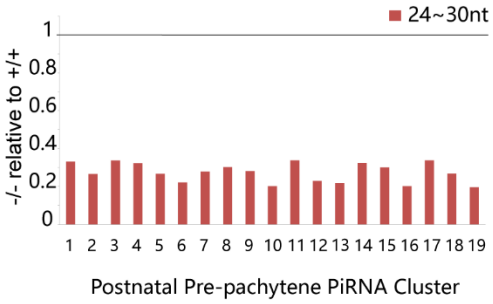
24~30nt
-/- relative to +/+
1
0.8
0.6
0.4
0.2
0
1 2 3 4 5 6 7 8 9 10 11 12 13 14 15 16 17 18 19
Postnatal Pre-pachytene PiRNA Cluster

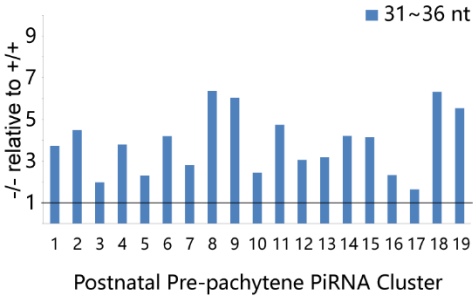
31~36 nt
-/- relative to +/+
9
7
5
3
1
1 2 3 4 5 6 7 8 9 10 11 12 13 14 15 16 17 18 19
Postnatal Pre-pachytene PiRNA Cluster

B

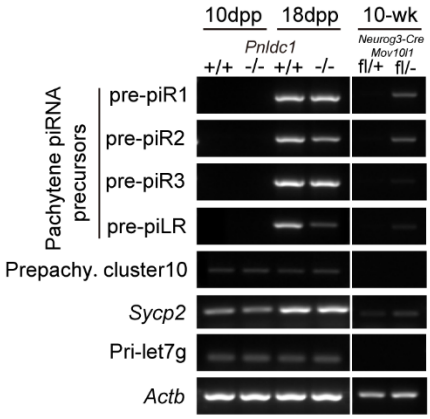
10dpp
18dpp
10-wk
Pnldc1
+/+ -/- +/+ -/-
Neurog3-Cre Mov10l1
fl/+ fl/-
Pachytene piRNA precursors
pre-piR1
pre-piR2
pre-piR3
pre-piLR
Prepachy. cluster10
Sycp2
Pri-let7g
Actb

C

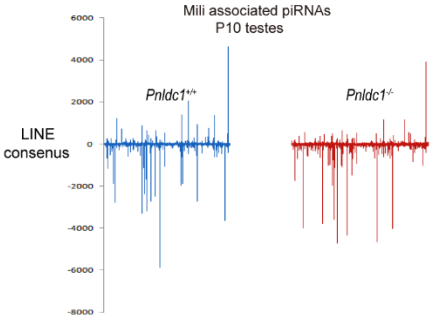
Mili associated piRNAs
P10 testes
LINE consenus
Pnldc1+/+
Pnldc1-/-
6000
4000
2000
0
-2000
-4000
-6000
-8000

Supplementary information, Figure S6. Compromised pre-pachytene piRNA biogenesis in P10 *Pnldc1*$^{-/-}$testes.

(A) Expression level of piRNAs derived from top 19 pre-pachytene piRNA clusters in P10 *Pnldc1*$^{-/-}$ total small RNA library relative to that in *Pnldc1*$^{+/+}$ library. Left: 24-30 nt total small RNA reads, right: 31-36nt total small RNA reads.

(B) RT-PCR analysis for four pachytene piRNA precursors transcripts (pre-piR1, pre-piR2, pre-piR3 and pre-piLR) and one pre-pachytene piRNA cluster (cluster 10) transcript. Pri-let7g, the precursor of microRNA let7g. Actb was used as a loading control.

(C) Reads mapped to transposon consensus of MILI associated RNAs from P10 mice.

A

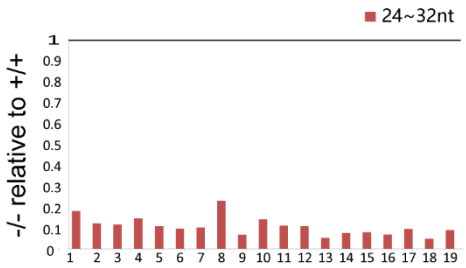
24~32nt
-/- relative to +/+
1
0.9
0.8
0.7
0.6
0.5
0.4
0.3
0.2
0.1
0
1 2 3 4 5 6 7 8 9 10 11 12 13 14 15 16 17 18 19

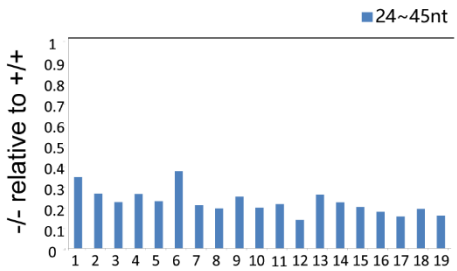
24~45nt
-/- relative to +/+
1
0.9
0.8
0.7
0.6
0.5
0.4
0.3
0.2
0.1
0
1 2 3 4 5 6 7 8 9 10 11 12 13 14 15 16 17 18 19

B

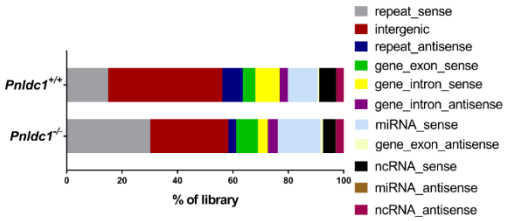
Pnldc1+/+
Pnldc1-/-
0 20 40 60 80 100
% of library
repeat_sense
intergenic
repeat_antisense
gene_exon_sense
gene_intron_sense
gene_intron_antisense
miRNA_sense
gene_exon_antisense
ncRNA_sense
miRNA_antisense
ncRNA_antisense

C

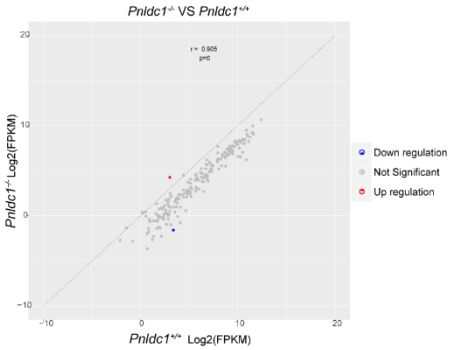
Pnldc1-/- VS Pnldc1+/+
r = 0.905
p=0
20
10
0
−10
−10 0 10 20
Pnldc1-/- Log2(FPKM)
Pnldc1+/+ Log2(FPKM)
Down regulation
Not Significant
Up regulation

Supplementary information, Figure S7. PNLDC is required for proper pachytene piRNA biogenesis in mice.

(A) Expression level of piRNAs derived from top 19 pachytene piRNA clusters in *Pnldc1*$^{-/-}$ total small RNA library relative to that in *Pnldc1*$^{+/+}$ library. Left: 24-32nt reads; right: 24-45nt reads.

(B) Genomic annotation of total small RNAs reads in P18 *Pnldc1*$^{+/+}$ and *Pnldc1*$^{-/-}$ testes.

(C) Relative abundance of 215 piRNA generating precursor transcripts in P18 *Pnldc1*$^{-/-}$ testes compared with age matched *Pnldc1*$^{+/+}$ testes.

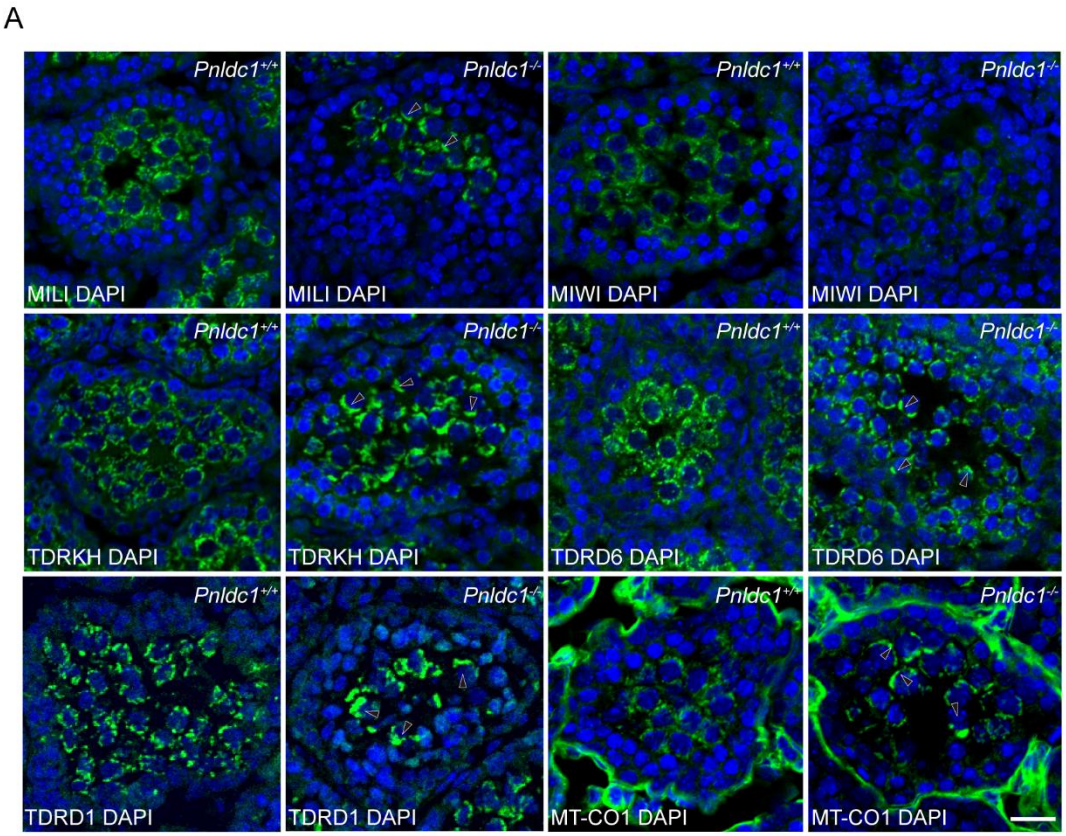
A
Pnldc1+/+
Pnldc1-/-
MILI DAPI
MILI DAPI
MIWI DAPI
MIWI DAPI
TDRKH DAPI
TDRKH DAPI
TDRD6 DAPI
TDRD6 DAPI
TDRD1 DAPI
TDRD1 DAPI
MT-CO1 DAPI
MT-CO1 DAPI

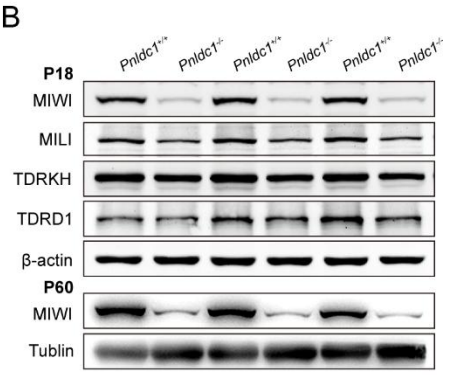
B
Pnldc1+/+
Pnldc1-/-
P18
MIWI
MILI
TDRKH
TDRD1
β-actin
P60
MIWI
Tublin

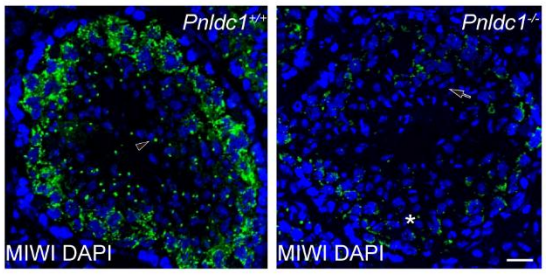
C
Pnldc1+/+
Pnldc1-/-
MIWI DAPI
MIWI DAPI

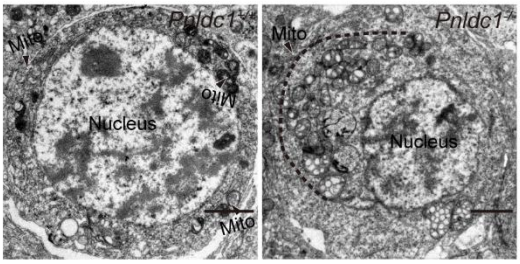
D
Pnldc1+/+
Pnldc1-/-
Mito
Mito
Nucleus
Mito
Mito
Nucleus

Supplementary information, Figure S8. Mislocalization of piRNA pathway components and mitochondria.

(A) Immunostaining of piRNA pathway components including MILI, MIWI, TDRKH and TDRD1 on frozen sections of P18 *Pnldc1*$^{+/+}$ and *Pnldc1*$^{-/-}$ testes. Immunostaining of MT-CO1, a component of mitochondrial respiratory chain complex IV, and TDRD6, a protein required for nuage formation. Scale bar, 20μm.

(B) Western blot analysis of abundance of piRNA pathway components in P18 and adult *Pnldc1*$^{+/+}$ and *Pnldc1*$^{-/-}$ testes.

(C) Immunostaining of MIWI on frozen sections of adult *Pnldc1*$^{+/+}$ and *Pnldc1*$^{-/-}$ testes. In round spermatids, MIWI localized in chromatoid body (arrowheads) in wild-type. In *Pnldc1* mutant, MIWI was still observed in chromatoid body of some round spermatids (asterisk), while absent in other round spermatids (arrows).Scale bar, 20μm.

(D) Electron micrographs of wild-type and *Pnldc1* deficient pachytene spermatocytes. Scale bar, 2μm.

Male fertility data from adult mice

Genotype	Age(wk)	n	Plugs	Fertility	Littersize
Pnldc1$^{+/+}$	8	3	100%(3/3)	100%(3/3)	7.66666667
Pnldc1$^{+/-}$	8	3	100%(3/3)	100%(3/3)	7.33333333
Pnldc1$^{-/-}$	8	3	0%(0/3)	0%(0/3)	0

Female fertility data from adult mice

Genotype	Age(wk)	n	Plugs	Fertility	Littersize
Pnldc1$^{+/+}$	8	3	100%(3/3)	100%(3/3)	7.66666667
Pnldc1$^{+/-}$	8	3	100%(3/3)	100%(3/3)	7.66666667
Pnldc1$^{-/-}$	8	3	100%(3/3)	100%(3/3)	8

Supplementary information, Table S1.

Fecundity of *Pnldc1*$^{-/-}$ males and females during a five-month mating period. [a*] Significantly different from result for both *Pnldc1*$^{+/+}$ and *Pnldc1*$^{+/-}$ mice ($P<0.05$).